nature structural & molecular biology

Structure of a ubiquitin-loaded HECT ligase reveals the molecular basis for catalytic priming

Elena Maspero[1], Eleonora Valentini[1], Sara Mari[1], Valentina Cecatiello[2], Paolo Soffientini[1], Sebastiano Pasqualato[2] & Simona Polo[1,3]

Homologous to E6-AP C terminus (HECT) E3 ligases recognize and directly catalyze ligation of ubiquitin (Ub) to their substrates. Molecular details of this process remain unknown. We report the first structure, to our knowledge, of a Ub-loaded E3, the human neural precursor cell–expressed developmentally downregulated protein 4 (Nedd4). The HECT^{Nedd4}~Ub transitory intermediate provides a structural basis for the proposed sequential addition mechanism. The donor Ub, transferred from the E2, is bound to the Nedd4 C lobe with its C-terminal tail locked in an extended conformation, primed for catalysis. We provide evidence that the Nedd4-family members are Lys63-specific enzymes whose catalysis is mediated by an essential C-terminal acidic residue.

Substrate ubiquitination occurs through an E1-E2-E3 Ub conjugation cascade. The E3 ligases play a crucial part in the whole pathway, as they determine the specificity of the reaction. Members of the HECT-type ligases receive Ub from the E2 through a thioester conjugate before catalyzing Ub transfer to their substrates[1]. The human genome encodes 28 HECT E3s, and a large number of them are involved in the genesis of several human diseases[2]. They are divided into subgroups according to the presence of interaction domains, although this classification probably does not reflect the natural evolution of these enzymes[3]. The Nedd4 family is a monophyletic group represented by nine members in humans and characterized by a C2 domain and three to four WW domains responsible for substrate recognition[4].

Structural studies on HECT domains revealed their architecture. The HECT is a bilobed domain consisting of an N-terminal N lobe that interacts with the E2 and a C-terminal C lobe that contains the catalytic cysteine and is free to rotate around the flexible hinge that tethers it to the N lobe[5]. Recent studies have demonstrated the existence and relevance of two Ub-interaction surfaces within the HECT domain. The first, present in the C lobe, is essential for E2-to-E3 Ub transfer[6]; the second, in the N lobe, is critical for enzyme processivity[7,8]. Notably, the ability to build up different Ub chains appears to be an intrinsic feature of the HECT domain[8–10]. The Nedd4 family of HECTs seems to use a sequential addition mechanism by which Ub molecules are added one at a time from the catalytic cysteine to the distal lysine of the growing chain[8,9]. However, most of the mechanistic details of HECT catalysis remain elusive, owing to the lack of structures of key catalytic intermediates.

To gain insight into the ubiquitination reaction catalyzed by HECT E3 ligases, we set out to determine the crystal structure of the Ub-loaded HECT domain of Nedd4 in complex with Ub noncovalently bound in the Ub-binding domain (UBD) present in the N lobe of HECT^{Nedd4} (ref. 8).

RESULTS

Structure of the HECT^{Nedd4}~Ub^{D}–Ub complex

Because a thioester-linked HECT~Ub is highly unstable, we generated a stable complex by bridging the HECT^{Nedd4} with a modified form of Ub donor (Ub^{D}), G76C, by a disulfide bond (**Supplementary Fig. 1a–d**). We solved the crystal structure of the complex (HECT^{Nedd4}~Ub^{D}–Ub) at 2.51-Å resolution by molecular replacement (**Table 1** and **Fig. 1a**). As predicted[8], loading of the Ub^{D} onto the HECT^{Nedd4} catalytic cysteine is compatible with noncovalent Ub binding in the N lobe. Furthermore, the N lobe adopts the same conformation in the presence and absence of Ub^{D} (r.m.s. deviation of 0.8 Å over 258 Cα), with free Ub kept in the binding site crafted by the N-lobe subdomains (**Supplementary Fig. 1e–g**). The N- and C-lobe organization markedly resembles that of the Nedd4-like HECT domain (HECT^{Nedd4L}) crystallized in complex with UbcH5B~Ub[6] (**Fig. 1b**, superposition with an r.m.s. deviation of 1.1 Å over 369 Cα), with the highly conserved N-lobe Tyr616 completely buried at the interface between the two lobes (**Fig. 1c** and **Supplementary Fig. 2**).

Notably, the Ub^{D} in the HECT^{Nedd4}~Ub^{D}–Ub structure sits in the same position as does the Ub loaded on the E2 in the HECT^{Nedd4L}–UbcH5B~Ub structure[6] (**Fig. 1b**). The main interaction surface is contributed by hydrophobic residues Leu71, Leu73, Ile36 and Pro37 of Ub^{D} and Leu861, Met888 and Ala889 of the C lobe, and it is surrounded by hydrogen bonds between Gln40 and the Leu861 main chain and between Asn892 and Leu8 and the Thr9 main chain, as well as by salt bridges between Asp39 and Lys860 (**Fig. 1d** and **Supplementary Fig. 3**). As the relative orientation between the two HECT lobes and between the C lobe and Ub^{D} in our structure is unchanged with respect to that described in another study[6], we conclude that our structure represents the step that immediately follows the transfer of the thioester bond from the E2 to the E3,

[1]Fondazione Istituto FIRC di Oncologia Molecolare, Milan, Italy. [2]Crystallography Unit, Department of Experimental Oncology, European Institute of Oncology, Milan, Italy. [3]Dipartimento di Scienze della Salute, Università degli Studi di Milano, Milan, Italy. Correspondence should be addressed to S. Polo (simona.polo@ifom.eu) or S. Pasqualato (sebastiano.pasqualato@ieo.eu).

Received 3 October 2012; accepted 21 March 2013; published online 5 May 2013; doi:10.1038/nsmb.2566

Table 1 Data collection and refinement statistics

	$HECT^{Nedd4}$~Ub^{D}–Ub	$HECT^{Nedd4}$ A889F
Data collection		
Space group	*R*32:h	*P*3121
Cell dimensions		
a, *b*, *c* (Å)	196.54, 196.54, 98.77	100.55, 100.55, 96.45
α, β, γ (°)	90, 90, 120	90, 90, 120
Resolution (Å)	56.74–2.51 (2.57–2.51)[a]	44.58–3.00 (3.10–3.00)[a]
R_{merge}	8.8 (88.5)	6.8 (69.7)
$I / \sigma I$	16.6 (2.9)	28.4 (3.9)
Completeness (%)	100.0 (100.0)	99.3 (99.1)
Redundancy	7.4 (7.5)	13.0 (12.4)
Refinement		
Resolution (Å)	56.74–2.51	44.58–3.00
No. reflections	22,567	11,550
R_{work} / R_{free}	18.4 / 22.9	24.6 / 29.5
No. atoms		
Protein	4,381	3,124
Water	112	3
B factors		
Nedd4 HECT domain	52.8	136.4
Ub^{D}	50.4	
Ub	82.3	
Water	46.1	93.9
r.m.s. deviations		
Bond lengths (Å)	0.008	0.003
Bond angles (°)	1.12	0.78

[a]Values in parentheses are for highest-resolution shell.

in which the Ub^{D} has been handed over to the C lobe and is ready to be transferred to the substrate.

Implications for the Ub^{D} C-terminal tail-locking

Differently from the aforementioned set of conserved contacts between Ub^{D} and the C lobe, the last three residues of Ub^{D} display a pronounced rearrangement with respect to the $HECT^{Nedd4L}$–UbcH5B~Ub structure, which locks the Ub tail in an extended conformation (**Fig. 2a**,**b**). The Ub^{D} tail zips onto C-lobe β-strand β9, just upstream of the catalytic Cys867, and organizes a hydrogen bond pattern that results in β-sheet augmentation, a common motif in protein-protein interactions[11]. Furthermore, Arg74, which is involved in a single hydrogen bond with residue Ser91 of UbcH5B in the E2-loaded conformation[6], folds back onto the C lobe and contributes two hydrogen bonds with the main chain carboxylic groups of Gln825 and Phe826 (**Fig. 2a**). We reasoned that these additional tail interactions may disfavor the reversibility of the thioester transfer, so that the thioester bond could not be handed back from the E3 to the E2. Owing to the involvement of backbone carbonyls, mutational analysis is precluded, but we note that R74A-mutated Ub^{D} was inefficiently released from the E2 in a pulse-chase assay[12].

A similar stretched conformation of Ub^{D} was recently observed in the RNF4–UbcH5A~Ub and BIRC7–UbcH5B~Ub structures[13,14], wherein the Ub tail was shown to orient the thioester bond, held on the E2 in an optimal conformation for nucleophilic attack by the incoming lysine residue of the substrate (**Fig. 2c**,**d**). Notably, the Ub-tail stretching has been reported also in the SUMO~RanGAP1–Ubc9–Nup358 complex[15], although in this case the crystal structure trapped the reaction product, with the protein modifier already transferred to the substrate (**Fig. 2e**). In the context of the $HECT^{Nedd4}$, the rigid configuration assumed by the C-terminal tail of Ub^{D} may ensure two important functions: it confers the directionality of the transthiolation reaction and, analogously to RNF4 and BIRC7, it facilitates acceptor recognition and optimizes the attack by the substrate lysine through the alignment of the thioester bond. Locking the flexible C-terminal tail of Ub in an extended conformation may be a common mechanism adopted by both E2s and E3s to prime the Ub^{D} for catalytic transfer to the substrate, though further structural studies are required to confirm this hypothesis.

Essential role of the Nedd4 C-terminal residue for catalysis

Close inspection of the sequence alignment of the HECT C-terminal tail revealed the presence of an invariable acidic residue as the last amino acid within the Nedd4 family (**Supplementary Fig. 4a**), suggesting that this might be a catalytic residue important in positioning and/or activation of the incoming lysine of the Ub acceptor (Ub^{A}). Indeed, mutations or even deletion of this single aspartic acid in Nedd4 supported this idea because it resulted in wild-type levels of transthiolation but completely undetectable ubiquitination (**Fig. 3a**,**b**). We obtained similar results assessing other Nedd4 family members: deletion of the last residue in Nedd4-like, Itch, Smurf2, WWP2 and Rsp5 abrogated substrate catalysis (**Fig. 3c**).

To test whether the C-terminal acidic residue could be in proximity to the catalytic site, we replaced it with a lysine. Consistently with previous mutational analysis, this single substitution abrogated Ub-chain formation (**Fig. 3d**). Notably, this terminal lysine was able to attack the thioesther bond, as demonstrated by the stoichiometric amount of Ub-modified HECT present in the reaction (**Fig. 3d**). MS analysis confirmed that the ubiquitinated peptide was the C-terminal one containing the diglycine-modified Lys900 (**Fig. 3e**). In contrast, no Ub modification of Lys900 was visible when we used the C867S catalytically impaired mutant, which proves that Lys900 did not attack the thioester-linked E2~Ub (**Fig. 3d**). Thus, upon correct positioning of the substrate or Ub^{A} the catalytic core is formed with the terminal acidic residue of Nedd4 located at the active site of catalysis. Once there, this acid residue may perform its still-undefined function, either contributing to the active catalytic site or helping to position the Ub^{A}. Further structures are needed to uncover its specific role.

Nedd4-family members are Lys63-specific E3 ligases

Our structure did not provide clues on the Ub^{A} position. Clearly, the Ub bound in the UBD present in the N lobe of $HECT^{Nedd4}$ does not represent the Ub^{A} carrying the attacking lysine (**Supplementary Fig. 1e**). Nedd4 is a Lys63-specific E3 ligase[8,9], and the UBD is not essential for chain specificity. Indeed, mutants in the critical residues required for Ub binding were defective in chain elongation but still retained Lys63 specificity[8]. Data from a previous study[9] have demonstrated that chain type specificity is an inherent property of the HECT domain itself and that the determinants of chain type specificity are located within the last 60 amino acids of the C lobe (**Supplementary Fig. 4b**). We extended this knowledge, performing absolute-quantification (AQUA) experiments on various HECTs of the Nedd4 family. Our data demonstrated that, with wild-type Ub as a source of Ub, all Nedd4-family members showed a clear preference for Lys63 linkage *in vitro* (**Fig. 4a**,**b**), although we failed to define a specific Lys63 sequence pattern by using a sequence conservation analysis (S. Polo and K. Hofmann, personal communication). Thus, we concluded that the Nedd4-family members are Lys63 specific and are characterized by a conserved and essential residue as the last amino acid.

Notably, other HECTs not belonging to the Nedd4 family do not have an acidic residue as the final amino acid (**Supplementary Fig. 4a**).

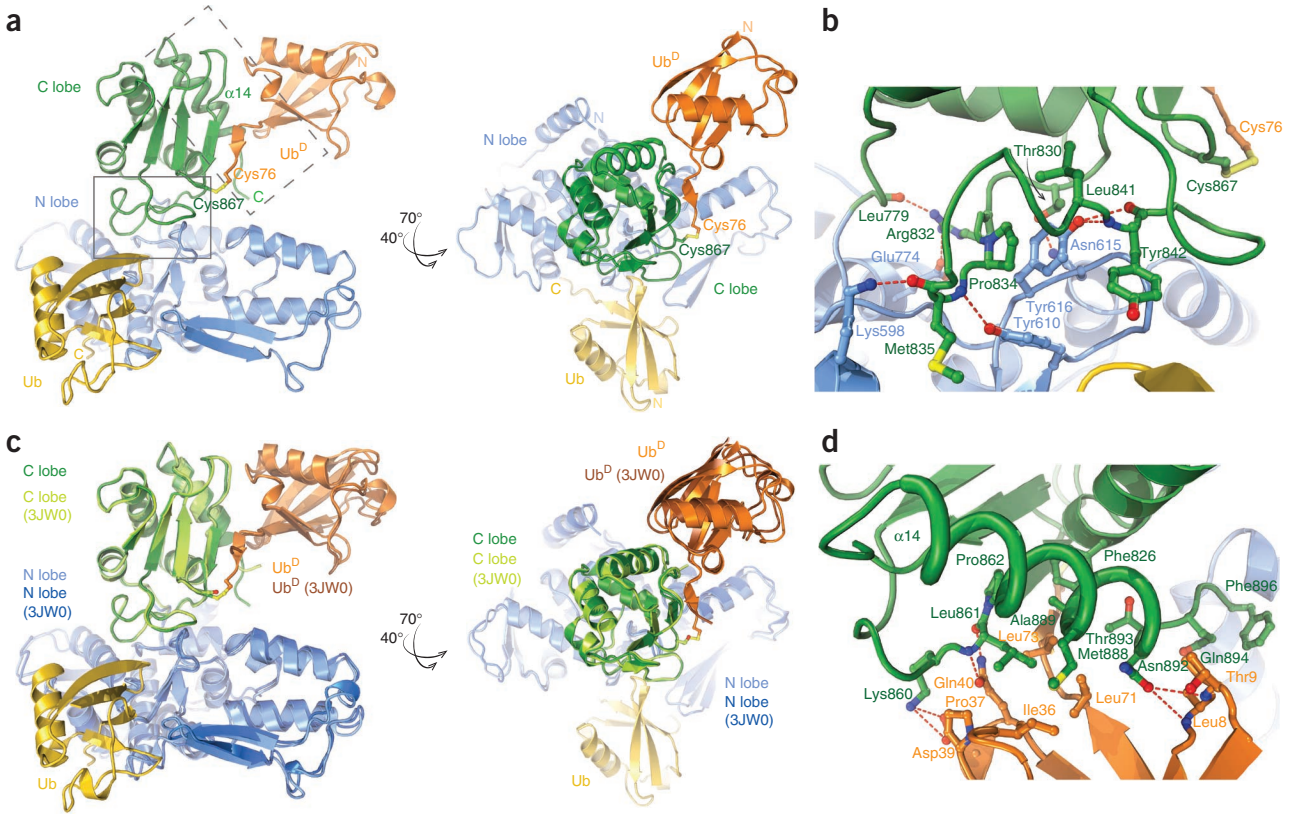

Figure 1 Structure of the Ub-loaded Nedd4 HECT in complex with Ub. (**a**) Cartoon representation of the HECT^{Nedd4}~Ub^{D}–Ub complex. Blue and green, N and C lobes, respectively; orange, Ub^{D}; yellow, noncovalently bound Ub. Right, same representation, rotated as indicated. (**b**) Cartoon representation of the superposition, done through their HECTs, of HECT^{Nedd4}~Ub^{D}–Ub with HECT^{Nedd4L}–UbcH5B~Ub (PDB 3JW0). UbcH5B is not shown, to permit a better view of the HECT and Ub superposition. Nedd4-like N and C lobes and loaded Ub are in dark blue, light green and brown, respectively; other molecules are colored as in **a**. (**c**,**d**) Details of the interaction between the C lobe in green and the N lobe in blue (**c**, corresponding to plain rectangle in **a**) and between HECT N lobe in green and Ub^{D} in orange (**d**, corresponding to dashed rectangle in **a**). Residues buried or participating at the interface are drawn in ball-and-stick representation and labeled. Hydrogen bonds are highlighted with red dashed lines.

Previous data indicated that E6AP preferentially synthesizes Lys48 chains[9,10]. Deletion of the last amino acid of E6AP did not affect its activity[16], which suggests a different catalytic mechanism. To gain insight into this difference, we substituted the last four residues after Nedd4 Phe896 with the three residues of E6AP. This short substitution showed reduced chain-formation kinetics (**Fig. 4c**), and the mutant was able to partially modify the type of the chains produced, as visualized by Lys63- and Lys48-specific antibodies (**Fig. 4d**). On the basis of these results, we concluded that the last three or four amino acids present in the C-terminal tail of the HECT ligases might participate, together with the determinants present in the C lobe[9], in determining chain specificity.

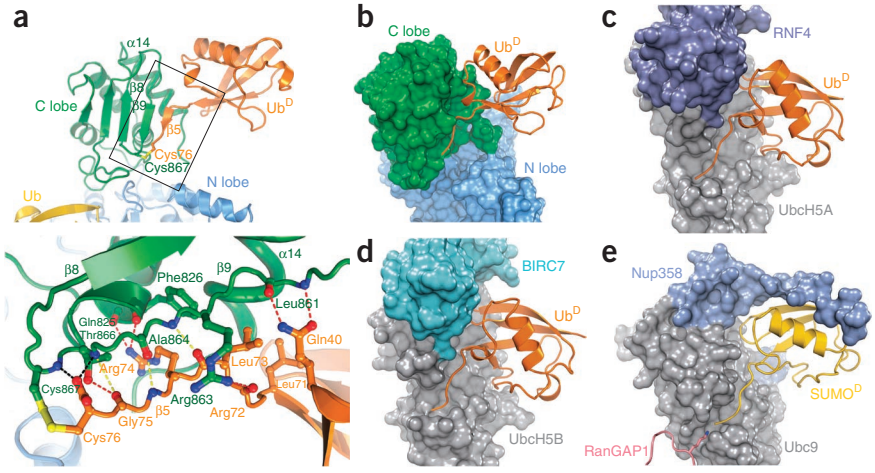

Figure 2 Ub^{D} is primed for catalysis by C-terminal tail-locking. (**a**) Details of the interactions at the interface between the HECT C lobe (green) and Ub^{D} (orange), as in **Figure 1c**. Hydrogen bonds between Cys76 carboxylate and backbone amides of Thr866 and Cys867, probably artificially imposed by the glycine-to-cysteine mutation in Ub, are shown in black. Hydrogen bonds in the β-sheet are shown in yellow. (**b**–**e**) Similar extended conformation of Ub or SUMO C-terminal tails, shown for Nedd4~Ub^{D} (this study) (**b**), RNF4–UbcH5A~Ub complex (PDB 4AP4) (**c**), BIRC7–UbcH5B~Ub complex (PDB 4AUQ) (**d**) and SUMO~RanGAP1–Ubc9–Nup358 complex (PDB 1Z5S) (**e**). E2 and E3 molecules are shown in surface representation, Ub, SUMO and RanGAP1 in cartoon representation.

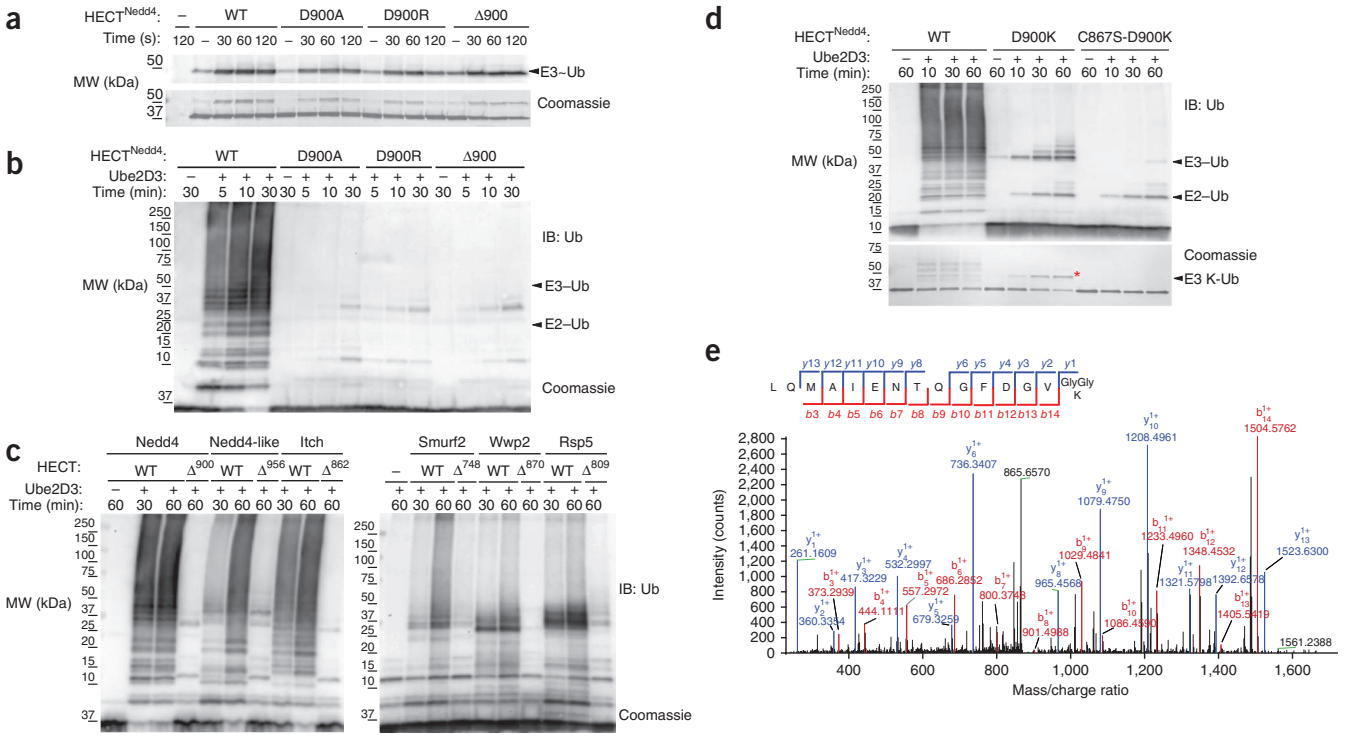

Figure 3 The C-terminal acidic residue is critical for the catalysis of Nedd4 family members. (**a**) Pulse-chase transfer of Ub from UbcH5B to the indicated HECT^{Nedd4} mutants. Top, streptavidin blot. HECT~Ub thioester is indicated. Bottom, Coomassie staining. WT, wild type. MW, molecular weight. (**b**–**d**) Ub chain formation assay with the indicated mutants and immunoblot (IB) of Ub. Arrowheads to monoubiquitinated E2 and E3 enzymes. Bottom, Coomassie staining. Red asterisk indicates the band of monoubiquitinated HECT cut for MS analysis. (**e**) MS/MS spectrum of the C-terminal peptide of Nedd4 D900K with the diglycine-modified lysine residue. Peptide sequence is shown with the annotation of the identified matched *b* ions in red and the *y* ions in blue.

Ala889 is critical for Nedd4 C-terminal tail-positioning

To test the functional importance of the Ub^D position for substrate ubiquitination, we examined various HECT mutants that elicit moderate catalytic effects in transthiolation reactions[6]. Ala889, which is conserved in all HECT ligases (**Supplementary Fig. 4a**), showed a notable behavior. Ala889 is buried largely within the C-lobe hydrophobic core, surrounded by Phe826, Leu861 and Pro862. Leu73 from Ub^D conceals the residual 5-Å^2 surface exposed to solvent (**Fig. 1c**). Mutations of Ala889 to other hydrophobic residues are unlikely to have a marked effect on the Ub^D position. Consistent with this, the transthiolation reaction occurred equally for the A889V, A889I and A889F variants. However, A889V and A889I mutants showed substantial impairment in chain elongation kinetics, whereas the A889F was a 'dead' mutant incapable of using Ub as a pseudosubstrate (**Fig. 5a**,**b**).

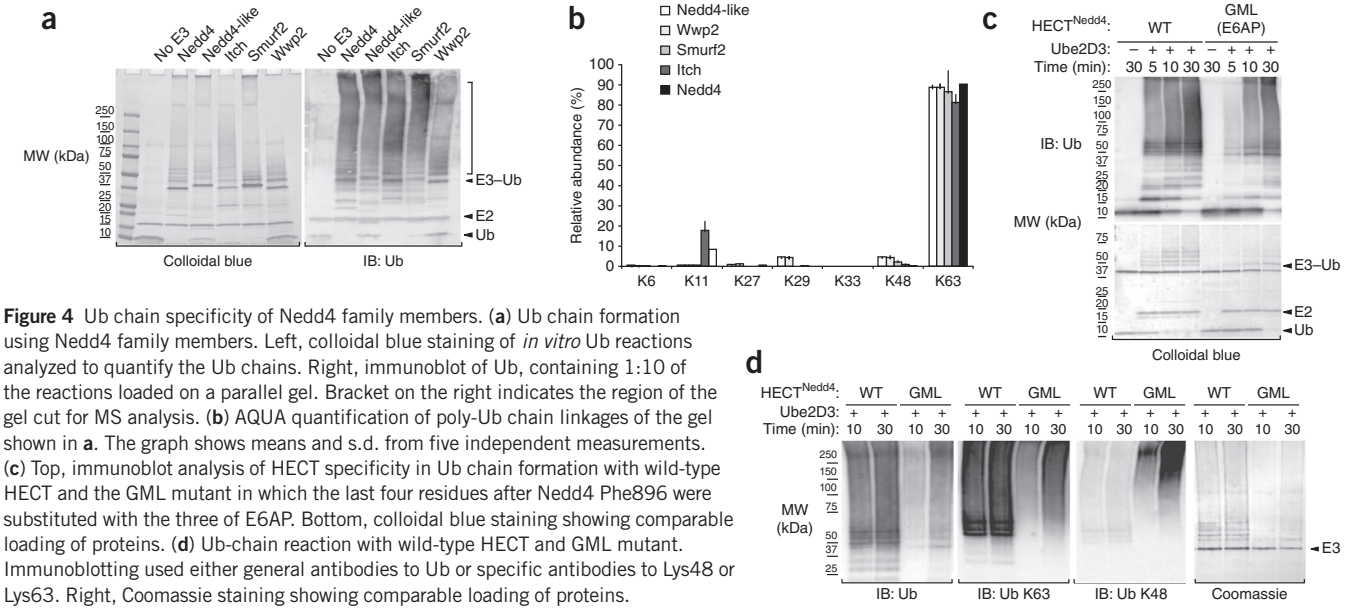

Figure 4 Ub chain specificity of Nedd4 family members. (**a**) Ub chain formation using Nedd4 family members. Left, colloidal blue staining of *in vitro* Ub reactions analyzed to quantify the Ub chains. Right, immunoblot of Ub, containing 1:10 of the reactions loaded on a parallel gel. Bracket on the right indicates the region of the gel cut for MS analysis. (**b**) AQUA quantification of poly-Ub chain linkages of the gel shown in **a**. The graph shows means and s.d. from five independent measurements. (**c**) Top, immunoblot analysis of HECT specificity in Ub chain formation with wild-type HECT and the GML mutant in which the last four residues after Nedd4 Phe896 were substituted with the three of E6AP. Bottom, colloidal blue staining showing comparable loading of proteins. (**d**) Ub-chain reaction with wild-type HECT and GML mutant. Immunoblotting used either general antibodies to Ub or specific antibodies to Lys48 or Lys63. Right, Coomassie staining showing comparable loading of proteins.

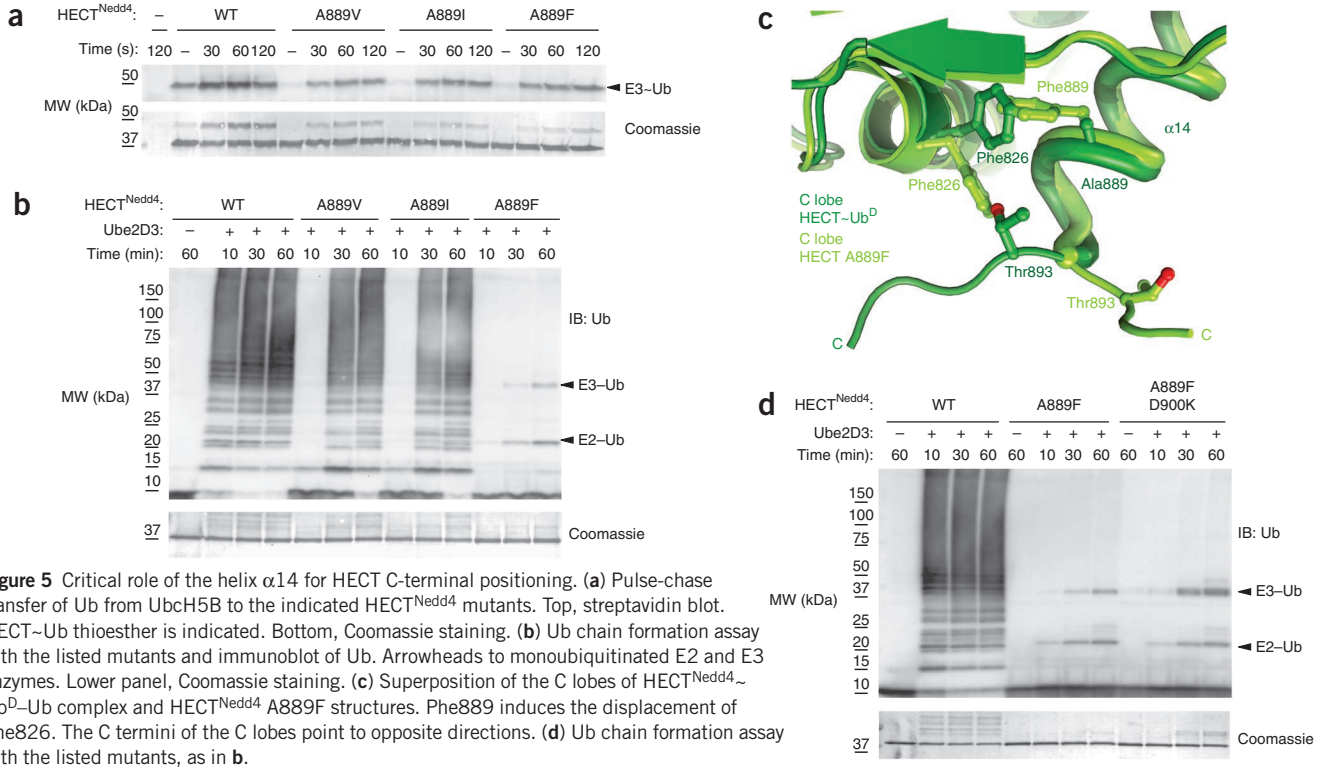

Figure 5 Critical role of the helix α14 for HECT C-terminal positioning. (**a**) Pulse-chase transfer of Ub from UbcH5B to the indicated HECT^{Nedd4} mutants. Top, streptavidin blot. HECT~Ub thioesther is indicated. Bottom, Coomassie staining. (**b**) Ub chain formation assay with the listed mutants and immunoblot of Ub. Arrowheads to monoubiquitinated E2 and E3 enzymes. Lower panel, Coomassie staining. (**c**) Superposition of the C lobes of HECT^{Nedd4}~Ub^{D}–Ub complex and HECT^{Nedd4} A889F structures. Phe889 induces the displacement of Phe826. The C termini of the C lobes point to opposite directions. (**d**) Ub chain formation assay with the listed mutants, as in **b**.

Ala889 sits in helix α14, just upstream of the C-terminal tail of the HECT. One possibility is that Ala889 is not required *per se* but rather functions to position the C-terminal tail during catalysis. To investigate this possibility, we solved the structure of the Nedd4 HECT domain carrying the A889F mutation (**Table 1**). The organization of the N and C lobes is different from those previously observed for HECT^{Nedd4} and closely resembles that adopted by the HECT domain of WWP1 (ref. 5 and **Supplementary Fig. 5a**). Mutation of Ala889 to phenylalanine does not induce any rearrangement in the structure of the C lobe, which superposes with that of HECT^{Nedd4}~Ub^{D}–Ub with an r.m.s. deviation of 0.6 Å over 111 Cα. The bulky side chain of Phe889 fills a hydrophobic pocket usually occupied by the Phe826 side chain, which is extruded from the C-lobe core and turned toward the C terminus (**Fig. 5c** and **Supplementary Fig. 5b**). This side chain extrusion, compatible with Ub^{D} loading, pushes the C-terminal tail far from the C-lobe core, owing to steric hindrance between the newly located Phe826 and Thr893 (**Fig. 5c**). Mutational analysis of Phe826 is precluded because this residue was previously shown to be critical for E2-to-E3 transthiolation[6]. Of note, substitution of Asp900 with lysine in the context of the A889F mutant did not result in Lys900-modified peptide as in the case of the wild-type HECT (**Fig. 5d**). On the basis of these results, we concluded that the incorrect positioning of the C-terminal tail is the primary cause of the catalytic defect of the A889F mutant.

DISCUSSION

The structure of the HECT^{Nedd4}~Ub^{D}–Ub complex offers the first glimpse, to our knowledge, of a Ub-loaded HECT primed for catalysis and, together with the biochemical data presented here, provides a framework for deciphering Lys63 specificity.

A key feature of the structure is the conserved noncovalent binding of the Ub^{D} to the HECT C lobe that is preserved after the transfer of the thioester bond from the E2 to the E3 (this study and ref. 6). This finding supports the notion that formation of a Ub chain requires cycling of the E3 between E2 and the substrate and is fully consistent with the sequential addition mechanism previously hypothesized for some HECT ligases: owing to steric hindrance, a Ub-loaded E2 enzyme is unable to access the C-lobe Ub-binding site until the E3 transfers its Ub^{D} to the substrate. Although molecular details may vary, Lys63 chain specificity together with sequence and structural conservation suggests that this catalytic mechanism may be general among the Nedd4 HECT–family members. This would not be necessarily true for other types of HECT ligases, such as E6AP, which is able to build a Lys48-linked chain on its HECT cysteine residue[10] and was recently suggested to carry two E2-binding sites[17]. These two features are indeed more compatible with the indexation or the seesaw models previously hypothesized[5,18].

An unresolved mystery of HECT catalysis is the role exerted by the conserved and essential phenylalanine residue[16] located most commonly at position –4 with respect to the C terminus of HECT (Phe896, position –5 in Nedd4; **Supplementary Fig. 4a**). We have been able to build this phenylalanine residue into the electron-density map (**Fig. 1d**). However, its location appears to be stabilized by interaction with a symmetry-related molecule, and it is probably not the one assumed during catalysis. We speculate that Phe896 will be positioned to exert its critical function only upon correct positioning of the substrate or the Ub acceptor. Its correct location will not necessarily be on the C lobe but possibly on an interface created by the correct orientation of the N and the C lobes. In the absence of the substrate, this binding site is not formed, as suggested by the fact that this residue has never been found ordered in HECT structures solved so far. This binding cleft should be conserved, because the phenylalanine residue is required in all the HECTs tested but has remained elusive because it is likely to be shaped only when the N and C lobes are organized with the substrate or the Ub^{A} in the catalytic position.

We were able to identify a second residue within the Nedd4 family, the acidic residue present at the extreme C terminus, exclusively required for the ligation step and not for the E3 thioester formation. On the basis of our mutational analysis (**Fig. 3**) we propose a speculative model about the possible catalytic mechanism adopted by Nedd4-family members. Upon correct positioning of the substrate or of the Ub acceptor in a growing chain, the catalytic core will be formed thanks to Phe896, which works as a pivot to guide the terminal residue of Nedd4 toward the active site of catalysis. However, the role of the −4 phenylalanine remains elusive. A definitive understanding of the ubiquitination process will require additional high-resolution structures of catalytic complexes of HECT and substrates and/or Ub chains.

METHODS

Methods and any associated references are available in the online version of the paper.

Accession codes. Coordinates for $HECT^{Nedd4}$~Ub^{D}–Ub complex and $HECT^{Nedd4}$ A889F have been deposited at the Protein Data Bank under accession codes 4BBN and 4BE8, respectively.

Note: Supplementary information is available in the online version of the paper.

ACKNOWLEDGMENTS

We thank P. Romano for critically reading the manuscript and for helpful discussions and advice and the staff at the European Synchrotron Radiation Facility and Swiss Light Source for assistance in data collection. This work was supported by grants from the Associazione Italiana per la Ricerca sul Cancro (AIRC, IG11627), the European Community (Network of Excellence FP6, 100601–201012) and the European Molecular Biology Organization Young Investigator Program to S. Polo. Access to the High Throughput Crystallization Laboratory of the European Molecular Biology Laboratory Grenoble outstation was funded by the European Community's Seventh Framework Programme (FP7/2007-2013) PCUBE (grant agreement 227764).

AUTHOR CONTRIBUTIONS

E.M. conducted the experiments with the help of E.V. and S.M.; V.C. assisted in crystallization; P.S. carried out MS analysis; S. Pasqualato performed structure determination and description; S. Pasqualato and E.M. participated in experimental design and data analysis; S. Polo conceived of the project, interpreted the results and wrote the paper.

COMPETING FINANCIAL INTERESTS

The authors declare no competing financial interests.

1. Scheffner, M., Nuber, U. & Huibregtse, J.M. Protein ubiquitination involving an E1-E2-E3 enzyme ubiquitin thioester cascade. *Nature* **373**, 81–83 (1995).
2. Scheffner, M. & Staub, O. HECT E3s and human disease. *BMC Biochem.* **8** (suppl. 1), S6 (2007).
3. Marín, I. Animal HECT ubiquitin ligases: evolution and functional implications. *BMC Evol. Biol.* **10**, 56 (2010).
4. Rotin, D. & Kumar, S. Physiological functions of the HECT family of ubiquitin ligases. *Nat. Rev. Mol. Cell Biol.* **10**, 398–409 (2009).
5. Verdecia, M.A. *et al.* Conformational flexibility underlies ubiquitin ligation mediated by the WWP1 HECT domain E3 ligase. *Mol. Cell* **11**, 249–259 (2003).
6. Kamadurai, H.B. *et al.* Insights into ubiquitin transfer cascades from a structure of a UbcH5B~ubiquitin-HECT(NEDD4L) complex. *Mol. Cell* **36**, 1095–1102 (2009).
7. Kim, H.C., Steffen, A.M., Oldham, M.L., Chen, J. & Huibregtse, J.M. Structure and function of a HECT domain ubiquitin-binding site. *EMBO Rep.* **12**, 334–341 (2011).
8. Maspero, E. *et al.* Structure of the HECT:ubiquitin complex and its role in ubiquitin chain elongation. *EMBO Rep.* **12**, 342–349 (2011).
9. Kim, H.C. & Huibregtse, J.M. Polyubiquitination by HECT E3s and the determinants of chain type specificity. *Mol. Cell Biol.* **29**, 3307–3318 (2009).
10. Wang, M. & Pickart, C.M. Different HECT domain ubiquitin ligases employ distinct mechanisms of polyubiquitin chain synthesis. *EMBO J.* **24**, 4324–4333 (2005).
11. Remaut, H. & Waksman, G. Protein-protein interaction through β-strand addition. *Trends Biochem. Sci.* **31**, 436–444 (2006).
12. Wang, M., Cheng, D., Peng, J. & Pickart, C.M. Molecular determinants of polyubiquitin linkage selection by an HECT ubiquitin ligase. *EMBO J.* **25**, 1710–1719 (2006).
13. Dou, H., Buetow, L., Sibbet, G.J., Cameron, K. & Huang, D.T. BIRC7–E2 ubiquitin conjugate structure reveals the mechanism of ubiquitin transfer by a RING dimer. *Nat. Struct. Mol. Biol.* **19**, 876–883 (2012).
14. Plechanovová, A., Jaffray, E.G., Tatham, M.H., Naismith, J.H. & Hay, R.T. Structure of a RING E3 ligase and ubiquitin-loaded E2 primed for catalysis. *Nature* **489**, 115–120 (2012).
15. Reverter, D. & Lima, C.D. Insights into E3 ligase activity revealed by a SUMO–RanGAP1–Ubc9–Nup358 complex. *Nature* **435**, 687–692 (2005).
16. Salvat, C., Wang, G., Dastur, A., Lyon, N. & Huibregtse, J.M. The -4 phenylalanine is required for substrate ubiquitination catalyzed by HECT ubiquitin ligases. *J. Biol. Chem.* **279**, 18935–18943 (2004).
17. Ronchi, V.P., Klein, J.M. & Haas, A.L. E6AP/UBE3A ubiquitin ligase harbors two e2~ubiquitin binding sites. *J. Biol. Chem.* published online, doi:10.1074/jbc.M113.458059 (25 February 2013).
18. Hochstrasser, M. Lingering mysteries of ubiquitin-chain assembly. *Cell* **124**, 27–34 (2006).

ONLINE METHODS

Reagents and constructs. Antibodies and their suppliers were: mouse monoclonal anti-Ub (ZTA10, generated in house, dilution 1:5); rabbit monoclonal anti-Lys48 and anti-Lys63 antibodies (clone Apu2 and Apu3, Millipore, dilution 1:1,000); streptavidin HRP and Imperial Protein Stain (Thermo Scientific). Biotinylated Ub was from Enzo Life Sciences. Bovine Ub was from Sigma-Aldrich. Nedd4 HECT–based constructs were engineered by site-directed mutagenesis. All other constructs were previously described[8,19]. All constructs were sequence-verified. Details are available upon request.

Protein expression and purification. GST fusion proteins were expressed in *E. coli* BL21 (DE3) at 18 °C for 16 h after induction with 500 μM IPTG at an OD_{600} of 0.5. Cell pellets were resuspended in lysis buffer (50 mM Na-HEPES, pH 7.5, 200 mM NaCl, 1 mM EDTA, 0.1% NP40, 5% glycerol and Protease Inhibitor Cocktail set III (Calbiochem)). Sonicated lysates were cleared by centrifugation at 20,000 r.p.m. for 45 min. Supernatants were incubated with 1 ml of glutathione-Sepharose beads (GE Healthcare) per liter of bacterial culture. After 4 h at 4 °C, beads were washed with PBS and equilibrated in cleavage buffer (50 mM Tris-HCl, pH 7.4, 100 mM NaCl, 1 mM EDTA, 1 mM DTT and 5% glycerol). To cleave off GST, 10 units of PreScission protease (GE Healthcare) per mg of substrate were incubated for 16 h at 4 °C.

Untagged Ub G76C mutant was expressed in BL21 (DE3) *E. coli* at 18 °C for 16 h after induction with 1 mM IPTG at an OD_{600} of 0.5. Cell pellets were resuspended in lysis buffer (25 mM ammonium acetate, 10 mM β-mercaptoethanol, 10% glycerol and protease inhibitors, pH 7.0) and lysed by sonication. Cell debris was removed by centrifugation, and the supernatant was adjusted to pH 4.5–5.0 with concentrated acetic acid. Precipitated proteins were removed by centrifugation, and the supernatant containing the Ub monomers was passed through a 0.45-mm PES filter. After dialysis, Ub was purified onto a Superdex 75 size-exclusion chromatography column equilibrated with 20 mM Tris-HCl, pH 8.0, 200 mM NaCl, 1 mM EDTA, 2 mM DTT and 5% glycerol. Bovine Ub was purified onto a Superdex 75 size-exclusion chromatography column equilibrated with 20 mM Tris-HCl, pH 8.0, 200 mM NaCl, 1 mM EDTA, 1 mM DTT and 5% glycerol.

$HECT^{Nedd4}$~Ub^{D} production. Cleaved $HECT^{Nedd4}$ was concentrated in Vivaspin concentrators (MW cutoff 30 kDa, Sartorius Stedim Biotech) and loaded onto a Superdex 200 size-exclusion chromatography column (GE Healthcare) equilibrated with 20 mM Tris-HCl, pH 8.0, 200 mM NaCl, 1 mM EDTA, 1 mM DTT and 5% glycerol. Fractions containing $HECT^{Nedd4}$ were collected, concentrated at 0.1 mM and incubated with 0.1 mM Ub G76C in the presence of 2 mM TCEP at room temperature for 30 min to fully reduce the cysteines. Formation of disulfide bonds was conducted essentially as described in ref. 20 with a dialysis treatment in disulfide-bond buffer (100 mM $Na_2HPO_4^-$ NaH_2PO_4, pH 7.5, 200 mM NaCl, 5% glycerol and 25 μM $CuCl_2$) at room temperature. Disulfide-bond formation was monitored by nonreducing SDS-PAGE until Ub G76C monomer depletion (48 h). The $HECT^{Nedd4}$~Ub complex was purified through a Resource Q anion-exchange column (GE Healthcare). Fractions containing pure $HECT^{Nedd4}$~Ub complex were confirmed by nonreducing SDS-PAGE, collected and concentrated (**Supplementary Fig. 1**). $HECT^{Nedd4}$~Ub and bovine Ub were mixed at a ratio of 1:2 and concentrated at 0.5 mM for subsequent crystallization studies.

Crystallization and structure determination. For the $HECT^{Nedd4}$~Ub^{D}–Ub complex, nanovolume crystallization screening experiments were performed at the High Throughput Crystallization Laboratory (HTX Lab) of the EMBL Grenoble outstation as described[21]. Crystals were reproduced in house in sitting drops in 96-well plates set up with a Honeybee Cartesian robot, with 37 mg/ml protein complex. Diffracting crystals were obtained at 4 °C in 2.4–2.6 M sodium malonate, pH 5.7–6.2. Crystals were harvested from the 96-well plate and directly vitrified in liquid nitrogen. Data were collected at the European Synchrotron Radiation Facility (Grenoble) on beamline ID14-4 at 0.9393 Å and 100 K. For $HECT^{Nedd4}$ A889F, initial hits were obtained by screening for crystallization conditions in sitting drops in 96-well plates set up in house with a Honeybee Cartesian robot. Diffracting crystals were grown at 20 °C in hanging drops in 24-well plates with 1.15 M potassium sodium tartrate, 100 mM Tris-HCl, pH 9.0, using protein at 10 mg/ml. Crystals were cryocooled in mother liquor supplemented with 10% ethylene glycol, and data collection was performed at beamline X06DA (PXIII) of the Swiss Light Source at the Paul Scherrer Institut, at 1.0000 Å and 100 K. All data were processed with XDS/XSCALE[22] within the automated data reduction system xia2 (ref. 23) or the automated go.com procedure available in house at beamline X06DA. The structures were solved by molecular replacement with Phaser[24] within the CCP4 suite[25], using Ub, N lobe and C lobe from PDB entry 2XBB. The models were improved by iterative cycles of manual building in Coot[26] and refinement with phenix.refine[27] and Refmac[28]. For $HECT^{Nedd4}$~Ub^{D}–Ub, 97.9% of residues are in the favored regions of the Ramachandran plot, and no residues are in the disallowed regions. For $HECT^{Nedd4}$ A889F, 97.0% of residues are in the favored regions and no residues are in disallowed regions.

Ubiquitination assays. All assays were performed in ubiquitination buffer (25 mM Tris-HCl, pH 7.6, 5 mM $MgCl_2$, 100 mM NaCl, 0.2 μM DTT and 2 mM ATP) with the HECT domain cleaved and purified as previously described and Ube2D3 as the E2 enzyme. Ube2D3 was produced as a His_6 fusion protein and purified by using Ni-NTA agarose beads (Qiagen, manufacturer's protocol) and size-exclusion chromatography. Bovine Ub (Sigma) was purified by size-exclusion chromatography.

For the transthiolation assay, the pulse-chase was performed in two steps. First, Ube2D3 (5 μM) was loaded with biotinylated Ub (10 μM) with E1 enzyme (100 nM) in ubiquitination buffer for 15 min at 37 °C and then quenched on ice by a two-fold dilution with 0.5 M EDTA. Then the loaded E2 was mixed with E3 $HECT^{Nedd4}$ in ubiquitination buffer to the following final concentrations: E2, 1.4 μM; Ub, 2.8 μM; E3, 1 μM. Thioester formation on the $HECT^{Nedd4}$ was monitored by quenching the reaction at different time points with Laemmli buffer without reducing agent. All mutants were assayed side by side with wild-type controls.

For the Ub chain formation assay, reaction mixtures (50 μl) containing purified enzymes (20 nM E1, 250 nM purified His_6-tagged Ube2D3 and 500 nM $HECT^{Nedd4}$) and 1.25 μM of Ub in ubiquitination buffer were incubated at 37 °C and stopped at the different time points by addition of 4× Laemmli buffer with reducing agent (100 mM DTT).

For Ub AQUA analysis, reaction mixtures (20 μl) containing purified enzymes (50 nM E1, 1.5 μM purified His_6-tagged Ube2D3 and 2.2 μM HECT) and 12.5 μM of Ub in ubiquitination buffer were incubated at 37 °C for 1 h and stopped by addition of 4× Laemmli buffer with reducing agent (100 mM DTT).

Mass spectrometry and quantitative analysis. Proteins were resolved by SDS-PAGE on a gradient gel (4–12% TGX Precast Gel, Bio-Rad) and stained with colloidal blue (Colloidal Blue Staining Kit, Invitrogen). Gel bands corresponding to Ub-modified HECT were digested with trypsin. Briefly, samples were subjected to reduction in 10 mM DTT for 1 h at 56 °C. Digestion was carried out by saturating the gel with 12.5 ng/μl sequencing-grade modified trypsin (Promega) in 50 mM ammonium bicarbonate overnight. Peptide mixtures were acidified with trifluoroacetic acid (TFA, final concentration 3%), extracted from gel slices with 30% acetonitrile (ACN)/ 3% TFA and concentrated to 100 μl in a vacuum concentrator. Peptides were loaded onto homemade C18-stage tips, dried and dissolved in 5% formic acid (FA) before analysis on the Agilent 1100 LC system (Agilent) coupled to Ultra LTQ-FT (Thermo Fisher Scientific). MS data were analyzed for protein identification and presence of diglycine signature by using Mascot considering the following parameters: Gly-Gly (K) +114.043 Da, Leu-Arg-Gly-Gly (K) +383.228 Da, peptide tolerance 10 p.p.m., MS/MS tolerance 0.5 Da.

For AQUA analysis, samples were directly dissolved with a solution of reference peptides for Lys6, Lys11, Lys27, Lys29, Lys33, Lys48 and Lys63 polyubiquitin branched chains (Cell Signaling Technology) in 5% formic acid. Samples were analyzed by using a range of reference-peptide concentrations spanning from 1 picomole to 100 femtomoles, injecting three technical replicates per concentration. All spectra were acquired in data-dependent mode. Ion chromatograms for reference and sample peptide-pair precursor ions were manually extracted with Xcalibur v1.4 (ThermoElectron). Chromatographic coelution of reference and endogenous peptide pairs and accurate peak integration were manually confirmed.

19. Woelk, T. *et al.* Molecular mechanisms of coupled monoubiquitination. *Nat. Cell Biol.* **8**, 1246–1254 (2006).
20. Serniwka, S.A., & Shaw, G.S. The structure of the UbcH8-ubiquitin complex shows a unique ubiquitin interaction site. *Biochemistry* **48**, 12169–12179 (2009).
21. Dimasi, N., Flot, D., Dupeux, F. & Marquez, J.A. Expression, crystallization and X-ray data collection from microcrystals of the extracellular domain of the human inhibitory receptor expressed on myeloid cells IREM-1. *Acta Crystallogr. Sect. F Struct. Biol. Cryst. Commun.* **63**, 204–208 (2007).
22. Kabsch, W. Xds. *Acta Crystallogr. D Biol. Crystallogr.* **66**, 125–132 (2010).
23. Winter, G. *xia2*: an expert system for macromolecular crystallography data reduction. *J. Appl. Crystallogr.* **43**, 186–189 (2010).

doi:10.1038/nsmb.2566

24. McCoy, A.J. *et al*. Phaser crystallographic software. *J. Appl. Cryst.* **40**, 658–674 (2007).
25. CCP4. The CCP4 suite: programs for protein crystallography. *Acta Crystallogr. D Biol. Crystallogr.* **50**, 760–763 (1994).
26. Emsley, P., Lohkamp, B., Scott, W.G. & Cowtan, K. Features and development of Coot. *Acta Crystallogr. D Biol. Crystallogr.* **66**, 486–501 (2010).
27. Adams, P.D. *et al*. PHENIX: a comprehensive Python-based system for macromolecular structure solution. *Acta Crystallogr. D Biol. Crystallogr.* **66**, 213–221 (2010).
28. Murshudov, G.N., Vagin, A.A. & Dodson, E.J. Refinement of macromolecular structures by the maximum-likelihood method. *Acta Crystallogr. D Biol. Crystallogr.* **53**, 240–255 (1997).